ACCOUNTS
of chemical research

Properties and Promises of Nanosized Insertion Materials for Li-Ion Batteries

MARNIX WAGEMAKER* AND FOKKO M. MULDER
Faculty of Applied Sciences, Delft University of Technology, The Netherlands

RECEIVED ON JULY 13, 2011

CONSPECTUS

The substantial influence of crystallite size on the properties of Li-ion storage materials has spurred intensive research in the emerging area of nanoionics. The development of nanoscale storage materials offers a promising strategy to increase the energy storage capabilities of Li-ion batteries, potentially making them suitable for electric vehicles. Nanosizing, which increases surface area, enhances the importance of interfaces and surfaces on directly observable materials properties such as the voltage profile and the phase diagram. As a result, nanosized materials can show improved storage properties, and materials inactive at the micro size can become excellent storage materials. We suggest novel surface storage mechanisms to explain these phenomena. First-order phase transitions, which are responsible for the batteries' constant voltage output, are partially suppressed at the nanoscale. So far the morphological changes during the phase transition remain unclear. A complete understanding of the equilibrium and non-equilibrium properties of a collection of nanosized electrode particles within an actual electrode remains a formidable challenge.

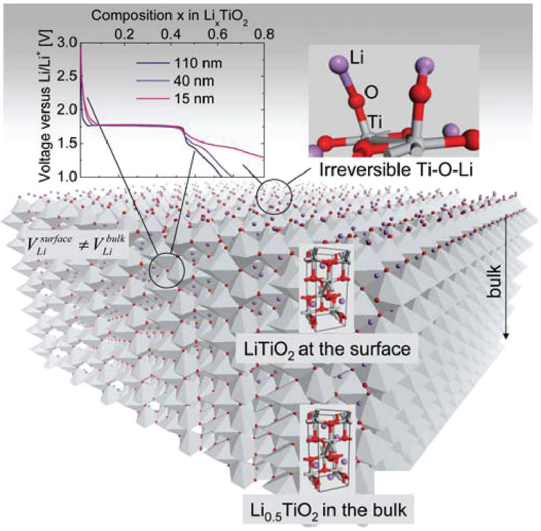

In this Account, we describe the efforts toward understanding the effects of nanosizing and its applications in representative insertion materials. We are particularly interested in the mechanisms and properties that will help to increase the energy storage of Li-ion batteries. We review and discuss the nanosize properties of lithium insertion materials, olivine $LiFePO_4$, and titanium oxides. Although nanosizing intrinsically destabilizes materials, which is potentially detrimental for battery performance, the relative stability of oxide and phosphate insertion compounds makes it possible to exploit the advantages of nanosizing in these materials. The larger capacities and typical voltage profiles in nanosized materials appear to be related to the surface and interface properties that become pronounced at the nanosize, providing a potential means of tailoring the material properties by particle size and shape.

The large irreversible capacity at the surface of some materials such as titanium oxides represents a disadvantage of nanosizing, but research is suggesting ways to resolve this problem. The changes in the first-order phase transition upon (de)lithiation could be related to the interface between the coexisting phases. At these interfaces, concentration gradients and strain lead to energy penalties, which significantly influence the thermodynamics of nanomaterial grains. However, it is less clear what nanoscaling effects predominate in the large collection of particles in actual electrodes. The complexity of these materials at the nanoscale and the difficulty in observing them in situ pose additional challenges. Future demands for stored electricity will require significant research progress in both nanomaterials synthesis and in situ monitoring.

1. Introduction: Energy Storage in Li-Ion Batteries

One of the main challenges of our society is the energy transition from fossil fuels toward renewable electricity sources such as wind and solar power. A key prerequisite for this transition is efficient electricity storage to facilitate the compensation of the difference in supply from renewable sources and the demand, and improvement of the stability of electrical grids. In addition, efficient electricity storage is required for electrical mobility for hybrid and electric vehicle applications.

Electrochemical storage is attractive, having very high storage efficiencies typically exceeding 90%, as well as

Published on the Web 02/10/2012 www.pubs.acs.org/accounts
10.1021/ar2001793

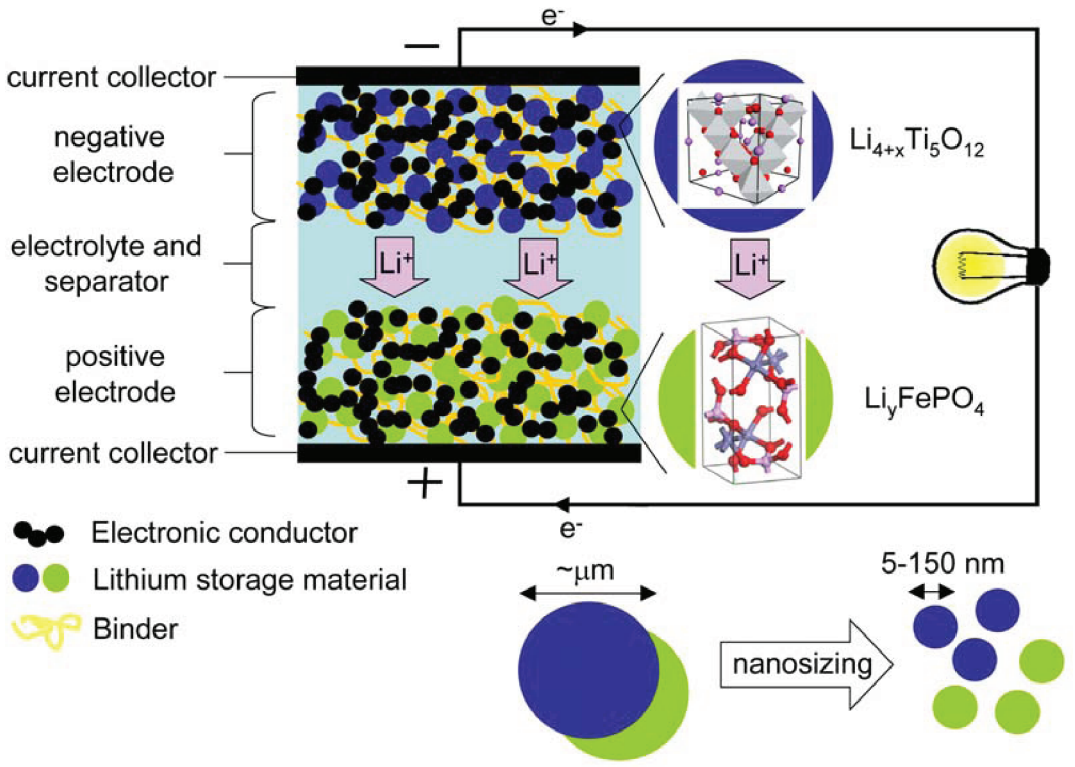

FIGURE 1. Schematic principle of a Li-ion battery.

relatively high energy densities. Application of Li-ion batteries in hybrid and electrical vehicles and static storage is emerging; however, improved performance and cost, combined with safety, are required. This has initiated worldwide research for Li-ion electrode materials that combine desirable properties such as high energy and power density, low cost, high abundance of elements, and electrochemical stability. In the current generation Li-ion batteries, insertion materials that reversibly host the lithium in the crystal structure form the most important class of electrodes. Although the future of Li-ion batteries looks bright, it should be noted that availability of a number of relevant transition metals and possibly lithium itself is a topic of interest.

In a Li-ion battery, two insertion material electrodes with a difference in lithium chemical potential (change in free energy upon Li addition) are in contact through an electrolyte (ionic conductor and electronic insulator), see Figure 1. The lithium will flow from the insertion material in which Li has a high chemical potential toward the electrode in which Li has a low chemical potential. Only Li ions can flow through the electrolyte, and the charge compensation electrons have to follow the Li ions via the external circuit, which can be used to power an application. By application of a higher electrical potential than the spontaneous equilibrium open circuit polarization, the process can be reversed. High energy density requires a large specific capacity of ions in both electrodes and a large difference in chemical potential. High power requires both electrons and Li ions to be highly mobile throughout the electrode materials and electrolyte.

It is generally assumed that the charge transport through the battery, both ionic and electronic, is limited by the electrode material. Typical insertion materials include transition metal oxides and phosphates, which are poor electronic conductors (semiconductors) and poor ionic conductors. Recent research has focused on nanosizing of electrode materials holding the promise of larger (dis)charge rates because it reduces the length of the rate-limiting diffusion pathway of Li-ions and electrons through the electrode material. The downside of the large surface area of nanostructured materials is the relative instability of nanomaterials promoting electrode dissolution and the increased reactivity toward electrolytes at voltages below 1 V vs Li/Li^+, which may adversely affect the Li-ion battery performance. Another potential disadvantage is the less dense packing leading to lower volumetric energy densities. Among the materials that benefit from the possibilities of nanosizing are the relatively stable transition metal oxides and phosphates operating well within the stability window of the electrolyte.

Numerous recent observations indicate that nanosizing electrode particles has large intrinsic impact on materials

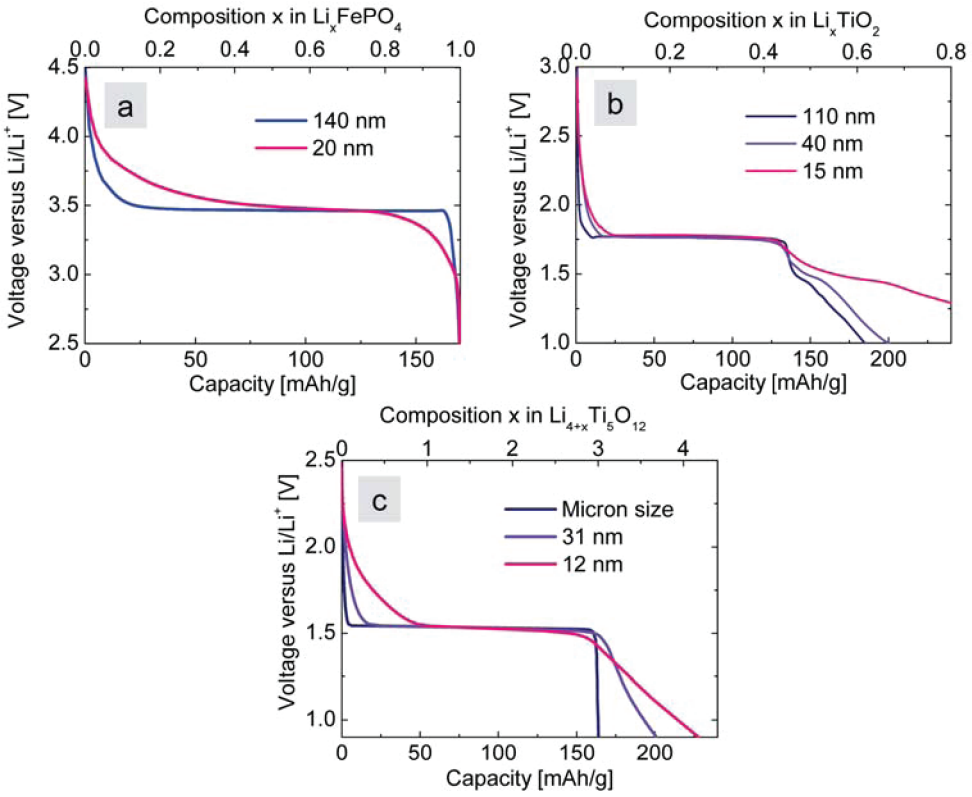

FIGURE 2. Voltage profiles of different particle sizes for Li_xFePO_4, anatase Li_xTiO_2, and spinel $Li_{x+4}Ti_5O_{12}$. Figure 2c reprinted with permission from ref 5. Copyright 2009 American Chemical Society.

properties[1,2] creating both opportunities and challenges for enhanced Li-ion storage. These observations include smearing out of the voltage profile[3−5] (see Figure 2), changing solubility limits and phase behavior[3,6−8] (see Figure 3), unexpected kinetics,[9] and larger capacities[7,10−13] (see Figure 2). The fundamental question is: are these changes simply due to the more abundant surface area and the trivial shorter diffusion distances, or does nanosizing additionally alter critical materials properties such as defect chemistry and thermodynamics in a nontrivial way? The practical question directly linked to the fundamental question is how these altered nanomaterial properties can be used to improve battery performance.

Recent year's observations in nanosized insertion materials for Li-ion batteries have led to much more insight into the impact of the nanosizing. However, it remains difficult to distill a coherent picture. This Account aims at bringing together recent observations in key insertion electrode materials in an attempt to formulate a coherent integrated picture of nanosize effects in insertion materials and their potential to improve battery performance. The materials discussed include olivine $LiFePO_4$ (positive electrode), anatase/rutile/brookite/bronze TiO_2, and spinel $Li_4Ti_5O_{12}$ (negative electrodes). The discussed size-dependent phenomena appear to be a general phenomenon for two-phase intercalation systems as indicated by results on Li_xTiO_2 and MgH_x systems.[7,14,15] We start by reviewing the nanosize effects of the individual electrode materials first, followed by a discussion integrating the observations, and a discussion of the potential application of nanoeffects to improve Li-ion battery performance.

2. Olivine Li_xFePO_4

Being chemically very stable and cheap Li_xFePO_4 ($0 < x < 1$), proposed by Padhi et al.[16] in 1997, has received considerable attention. Upon charging, a first-order phase transition occurs by nucleation of the Li-poor $Li_{x_\alpha}FePO_4$ triphylite in the Li-rich $Li_{x_\beta}FePO_4$ heterosite phase where $x_\alpha \approx 0$ and $x_\beta \approx 1$. The two-phase equilibrium is responsible for the constant voltage during (dis)charge in large particles as shown in Figure 2a. The initial hurdle of poor intrinsic electronic conduction was overcome using small particles in combination with conductive phases.[17,18] The next improvement, further nanosizing in combination with ionic conducting phases, resulted in unexpectedly fast kinetics.[19] This raised the question whether the nanosize improvements are caused by intrinsic changes in material properties or are simply due to the shorter diffusion distances through nanosized solid state.

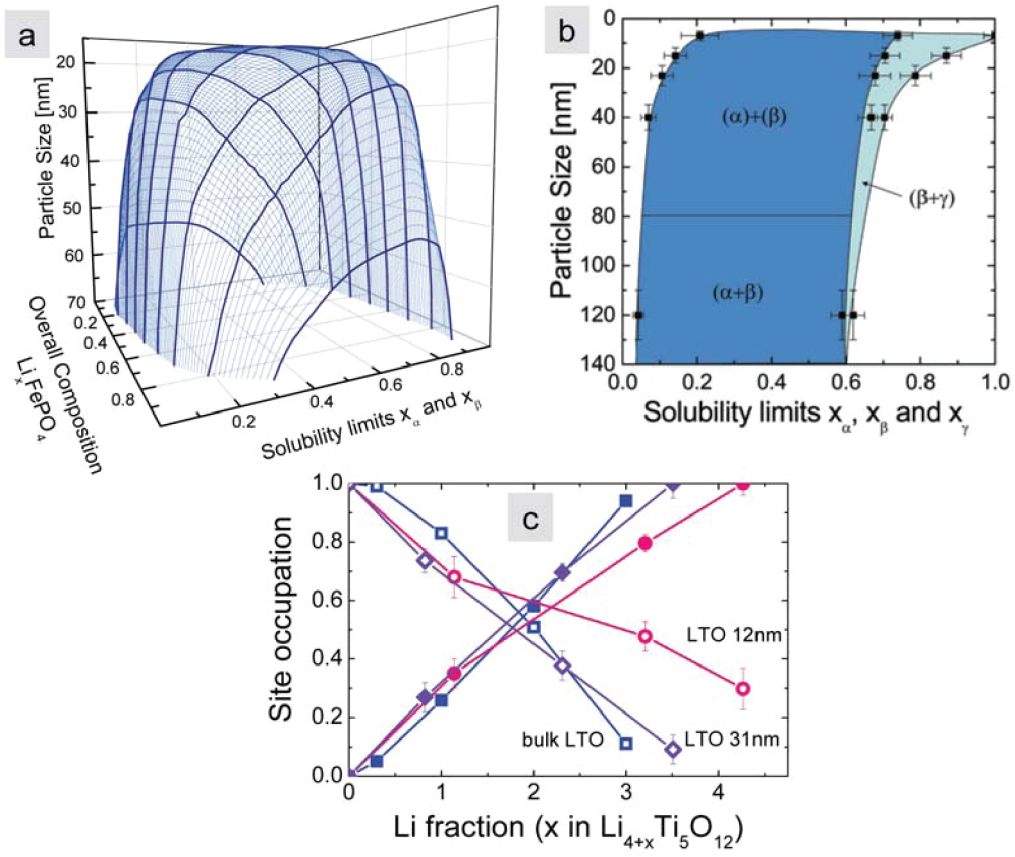

FIGURE 3. The structural impact of nanosizing in the various insertion materials determined by neutron diffraction. (a) Calculated solubility limits in olivine Li_xFePO_4 based on the diffuse interface in excellent agreement with the diffraction data.[8] (b) Solubility limits in anatase Li_xTiO_2 where α, β, and γ represent anatase, lithium-titanate, and $LiTiO_2$ respectively. $(\alpha) + (\beta)$ and $(\alpha + \beta)$ refer to the situation that each particle either has phase α or β and that both phases coexist within one particle, respectively. (c) Li occupancy of the 8a (closed symbols) and 16c (open symbols) sublattices in spinel $Li_{4+x}Ti_5O_{12}$. Reprinted with permission from ref 5. Copyright 2009 American Chemical Society.

Down sizing $LiFePO_4$ crystallites has a noticeable effect on the (dis)charge voltage profile as observed in Figure 2a. Explanations for the distribution of voltages in literature are (1) a reduction of the miscibility gap for smaller particle sizes due to strain,[20] surface energy,[21] and the (diffuse) interface energy[8,22] and (2) a distribution of voltages due to a distribution in nanoparticle size.[23,24]

(1) The solubility limits during the insertion reaction in $LiFePO_4$ have been under intensive research,[3,6,20−22,25−28] demonstrating narrow solid solution domains ($x_\alpha \approx 0$ and $x_\beta \approx 1$) in micrometer size particles at room temperature[27] and a solid solution over the entire compositional range above 520 K.[25,29] Yamada et al.[27] reported extended solid−solution composition ranges in small particles, and a systematic decrease of the miscibility gap was suggested due to strain based on Vegard's law.[3] Kobayashi et al.[6] isolated solid−solution phases, also supporting a size-dependent miscibility gap. Theoretical work indicates the importance of the diffuse interface,[22] strain,[20,30] and interface energy,[21] all increasing the energy of the coherent interface between the coexisting phases as shown schematically in Figure 5. Burch et al.[22] showed that in theory a coherent but compositional diffuse interface is able to destabilize the two-phase coexistence, predicting a size-dependent miscibility gap.[22] The diffuse interface also appears an essential ingredient for the prediction[31] of the experimentally observed layer-by-layer intercalation in $LiFePO_4$[32−34] (domino-cascade model[32]), although this model predicts that the diffuse interface is not observed. Recently it was shown that the diffuse interface also predicts the observed composition dependence of the miscibility gap, which is observed below particle sizes of 35 nm.[8] The resulting calculated phase-size diagram is shown in Figure 3a. These results indicate that in the nanoscale phases are not independently established but linked through their mutual interfaces and

require Li transport between the two phases when the overall composition changes by (dis)charging.

(2) Surface free energies become increasingly important in affecting voltage profiles as electrode particles approach nanometer dimensions. The plateau voltage of a first-order phase transformation depends on crystallite dimensions[23,24] as demonstrated schematically in Figure 6. A distribution of crystallite sizes consequently leads to a spectrum of transformation voltages that produces a sloping voltage profile similar to that of a solid solution,[23,24]also explaining the observations in Figure 2.

3. Li_xTiO_2 (Anatase, Rutile, TiO_2(B), and Brookite)

The inherent safety and stability of titanium oxides working at potentials around 1.5 V toward the electrolyte make these materials attractive candidates for the negative Li-ion electrodes, albeit with a loss in battery energy density. These materials show great promise[10−12,35,36] in particular upon nanosizing, having increased reaction areas, shortened Li-ion diffusion paths, and enhanced Li solubility and capacity. Several polymorphs exist, the most common in relation to lithium storage being anatase, rutile, bronze B, and brookite. Here we review these phenomena explicitly illustrated by anatase, but continuously referring to analogous observations in other polymorphs.

The altered voltage and phase properties shown in Figures 2b and 3b indicate that the thermodynamics of insertion in anatase is strongly affected by the crystal particle size.[4,7,10,15,35] The increase of the surface area has profound impact on the storage properties. A different Li-storage mechanism appears to occur at the surface[7] leading to the composition $LiTiO_2$, fully utilizing the $Ti^{3+/4+}$ redox couple, not observed in bulk material. Figure 3b shows that a particle size of 7 nm can completely be transformed toward tetragonal $LiTiO_2$. Down to ∼3 nm deep, the surface allows lithium storage exceeding the orthorhombic $Li_{\sim 0.5}TiO_2$ composition, which is responsible for the larger reversible (dis)charge capacities observed,[4,11] illustrated by Figure 2b. Similarly, in TiO_2(B),[12] rutile,[10] and brookite,[37] the storage capacity increases with decreasing particle size, suggesting similar surface environment enhanced Li storage. Also consistent with such a surface storage mechanism is the observation of pseudocapacitive behavior in TiO_2(B).[38]

The impact of size is immediately visible in Figure 2b where the voltage profile is shown for different particle sizes of anatase TiO_2. The region where the voltage is constant reflects the first-order phase transition from Li-poor anatase $Li_{x_a \approx 0.025}TiO_2$ to Li-rich lithium-titanate $Li_{x_b \approx 0.5}TiO_2$,[39,40] consistent with the phase−size diagram[7] in Figure 3b at large particle sizes. A remarkable observation is that the Li-ion solubility in the various phases depends systematically on the crystal particle size, shifting the miscibility gap rather than decreasing it. The 120 nm anatase crystals can host approximately Li/Ti = 0.03; however, the 7 nm particles are able to host up to Li/Ti = 0.21 while maintaining the anatase structure. The disappearance of the voltage plateau for smaller particle sizes has been related to these changing solubility limits.[4,7] The more curved shape of the voltage profile for nanosized materials appears to be a general phenomena in the various TiO_2 polymorphs such as rutile,[10] TiO_2(B),[12] and brookite,[37] and also the higher Li-ion solubility has been observed in nanostructured rutile,[41] suggesting that similar size effects play a role in these materials.

Another interesting observation is the different phase behavior in particle sizes above and below ∼80 nm referred to as $(\alpha + \beta)$ and $(\alpha) + (\beta)$ in Figure 3b. Large particles appear to be able to host both phases within one crystallite; small particles have either the Li-poor anatase or lithium-titanate phase. The origin of this was suggested to be the prevention of intraparticle coexisting phases and the associated phase boundary, that is, preventing the resulting energy penalty due to interface energy and strain. The absence of the interface rules out the interface energy effects on the solubility limits as discussed for $LiFePO_4$. However, here the shift in solubility observed in Figure 3b is fully consistent with the impact of surface energies as shown in Figure 6.

Upon nanosizing, all TiO_2 polymorphs suffer from a substantial irreversible capacity loss on the first cycle that appears to scale with the surface area,[4,10,12,38,42] compromising the use of nanostructured materials. Generally, the irreversible capacity loss is attributed to trapped lithium in the host structure[43] or decomposition of the electrolyte and SEI formation.[44] However, titanium oxide surfaces are well-known for H_2O and OH physisorption and chemisorption, forming strong Ti−O−H type bonds. We have shown that this explains the irreversible capacity loss by the formation of Ti−O−Li at the surface of amorphous TiO_2 where Li^+ exchanges with H^+, which reduces the electrolyte.[42]

4. Spinel $Li_4Ti_5O_{12}$

In 1994, Ferg et al. first described the possible application of this compound as an electrode material in a secondary Li-ion

battery.[45] The disadvantage of a high voltage of ~1.55 V versus Li metal compared with anode materials like graphite is compensated by the material's safe operation, high rate capability, low cost, and excellent recyclability. The latter is attributed to the minimal decrease in unit cell volume of only 0.2% between both members $Li_4Ti_5O_{12}$ and $Li_7Ti_5O_{12}$. In $Li_4Ti_5O_{12}$, abbreviated LTO, all tetrahedral 8a sites are occupied by lithium, resulting in $(Li_3)_{8a}[Li_1Ti_5]_{16d}(O_{12})_{32e}$. Upon Li insertion, the 16c sites are gradually filled and the 8a sites emptied, resulting in the end composition $[Li_6]_{16c}$-$[Li_1Ti_5]_{16d}(O_{12})_{32e}$. This process takes place with a very constant potential over almost the complete capacity, which is generally attributed to a two-phase coexistence of the end members during insertion.[46−48] Although during insertion this picture is correct, it has been demonstrated that in micrometer sized $Li_{4+x}Ti_5O_{12}$ two-phase separation is unstable above 80 K[49] and domains of 16c occupation and 8a occupation intimately mix at a nanometer length scale.[50] This appears as a solid solution for diffraction and the open circuit potential.[49] The structural relaxation may be rationalized by the zero-strain property. The very low interface and strain energy imposed by the coexisting phases facilitates mixing of the two phases on a small scale. This leads to a solid solution electrochemical response at relative low temperatures (above 80 K). In this context the zero-strain property of LTO is very interesting because it offers the possibility to study nanosize effects in the absence of strain and interface energy, unlike the previously discussed materials.

Particle size dependent electrochemical properties of the LTO spinel were systematically investigated by Kavan et al.[51] Using LTO particles ranging from 1 μm to 9 nm in thin electrode films, they found an optimum battery performance for particles at ~20 nm (~100 m^2/g) at a voltage interval of 2.5−0.9 V. Of additional interest is the presence of lithium compositions larger than $Li_7Ti_5O_{12}$ when the applied potential is as low as 0.01 V.[52] This is corroborated by *ab initio* calculations[53] showing that it is possible to obtain an 8a Li occupation in an all 16c framework up to a theoretical composition of $Li_{8.5}Ti_5O_{12}$. However, additional lithium incorporation was predicted to lead to a negative and therefore impossible to achieve intercalation potential. Recently we directly observed an increased capacity at positive potential with decreasing particle size, exceeding $Li_7Ti_5O_{12}$ (Figure 3c). Neutron diffraction proved simultaneous occupation of both 8a and 16c, which explains the additional capacity. Furthermore, the additional capacity was suggested to reside mainly near the surface, explaining the increasing capacity with decreasing particle size.[5] The observed distortion of the TiO_6 octahedra effectively screens the Coulomb repulsion between 8a and 16c Li^+ charges, lowering the energy. Apparently such distortion is energetically more favorable near the oxygen-terminated surface compared with the bulk, making significant simultaneous occupation of 8a and 16c only possible near the surface. Such oxygen-rich surfaces would also explain the relative high voltages of the first inserted capacity as well as the additional capacity at low potential that scales with the particle surface. However, too high surface lithium storage was found to result in irreversible capacity loss, most likely due to surface reconstruction, creating a thin layer of inactive material.[5,59] This rationalizes the existence of an optimal particle size[5] since such loss becomes relatively more important for smaller particle sizes.

5. Discussion: Size Effects

Direct evidence of the impact of particle size on the thermodynamics of nanoinsertion materials is the change in the solubility limits. In $LiFePO_4$[3,6,8] the reduction of the miscibility gap appears to result from the interface between the two end members, being the consequence either of strain,[3] of interface energy[21] or of the diffuse interface[8] The diffuse interface additionally explains the varying solubility limits that are observed with varying overall composition x in nano-Li_xFePO_4.

A prerequisite for the interface effects discussed is the presence of coexisting phases during (dis)charge. Although the interfaces are directly observed in chemically lithiated materials,[8,33,34] they are claimed to be absent under electrochemical conditions,[32] keeping the two-phase transition mechanism shown in Figure 4 under debate. In anatase TiO_2, the solubility limits shift to higher compositions with decreasing particle size as observed in Figure 3b, indicating a different mechanism. Particles below 40 nm were observed to have either the Li-poor or the Li-rich phase, corresponding to the right-hand mechanism in Figure 4, avoiding intraparticle phase boundaries altogether. In this case, a surface effect, involving a lower surface energy of the anatase phase than for the titanate phase, delays the formation of the latter in small particles,[24] resulting in high Li solubility in anatase.

The battery voltage is related to the difference in the chemical potential between the cathode and the anode according to

$$V = -(\mu_{Li}^{cathode} - \mu_{Li}^{anode})/e \quad (1)$$

Therefore, also the voltage profiles in Figure 2 demonstrate that in all materials discussed, nanosizing has a

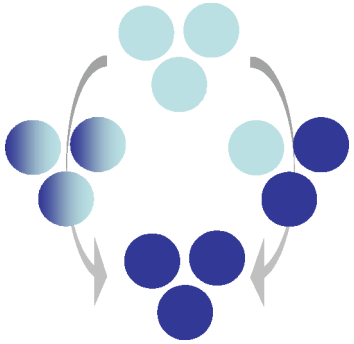

FIGURE 4. The two possible mechanisms for a first-order phase transition induced by Li-insertion in a collection of three electrode particles.

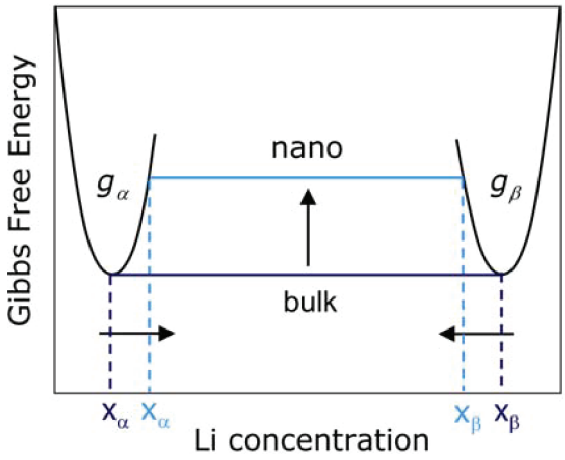

FIGURE 5. Schematic impact of an energy penalty due to the interface between the coexisting phases for materials that exhibit first-order phase transitions upon (de)lithiation. The interface energy (including strain and the diffuse interface) leads to an energy penalty raising the Gibbs Free energy thereby reducing the miscibility gap.

marked impact on the thermodynamics of insertion materials that exhibit a first-order phase transition. This Account brings forward several explanations for differences, the validity of which we will discuss here.

(1) Because the constant voltage is indicative of the first-order phase transition, the reduction of the composition domain where the voltage is constant, as observed in Figure 2, is associated with a reduction of the miscibility gap.[3,6] However, this does not explain the curved shape of the voltage curve indicating a different distribution of chemical potentials in, e.g., Figure 2c.

(2) Another eligible explanation is the distribution in particle sizes resulting in a distribution of voltages,[24] schematically illustrated by Figure 6. Often the relative width in the particle size distribution is larger for smaller particle size. However, also in the case of a narrow particle size distribution, as is the case for LTO in Figure 2c, the typical curved voltage is present.

(3) A fundamental thermodynamic origin of the curved voltage profile is the smearing of the first-order phase transition as the result of configurational entropy.[54] However, this effect can only be expected to become significant for systems smaller than ~1000 atoms, which, considering 1000 Li atoms in $LiFePO_4$, corresponds to systems smaller than ~4 nm. This appears consistent with the reported very small (approximately millivolt) hysteresis in equilibrium voltage curves due to this configurational entropy.[55]

(4) A final factor is revealed by LTO in which the chemical potential, and hence the insertion voltage, is suggested to be different at the surface.[5] Depending specifically on the orientation of the surface, the voltage can be expected to change gradually toward the bulk voltage over a distance of nanometers, as strengthened by our recent calculations of Li-ion storage at the oxygen-terminated surface of LTO.[56] This implies the curved voltage profile to be a consequence of the near surface environment, also explaining why the amount of capacity of the curved part of the voltage profile scales with the particle surface area.[5] Figure 7 schematically shows the insertion process that we suggest to occur in LTO: upon lithium insertion first the low chemical potential (high voltage) surfaces are inserted above the voltage plateau, followed by the bulk having the plateau chemical potential and finally the high chemical potential (low voltage) surfaces are charged. Also $LiFePO_4$ surface calculations illustrate that the chemical potential at the surface generally differs from the bulk chemical potential, either being larger or smaller, depending on the specific surface. Finally, also in anatase TiO_2 the reactivity appears to depend on the surface orientation.[57] In conclusion, we anticipate that in nanosized insertion materials lithium insertion near the surface is responsible for more favorable and less favorable insertion sites, yielding more curved voltage profiles. We speculate that this is the dominant contribution to the deviation from the potential plateau values in insertion materials. Interestingly, this suggests that shape and size of nanosized particles can, to a certain degree, be used to tailor the voltage profile and hence the storage properties.

The surface specific lithium storage properties also form a rationale for the higher capacities in anatase TiO_2 and LTO

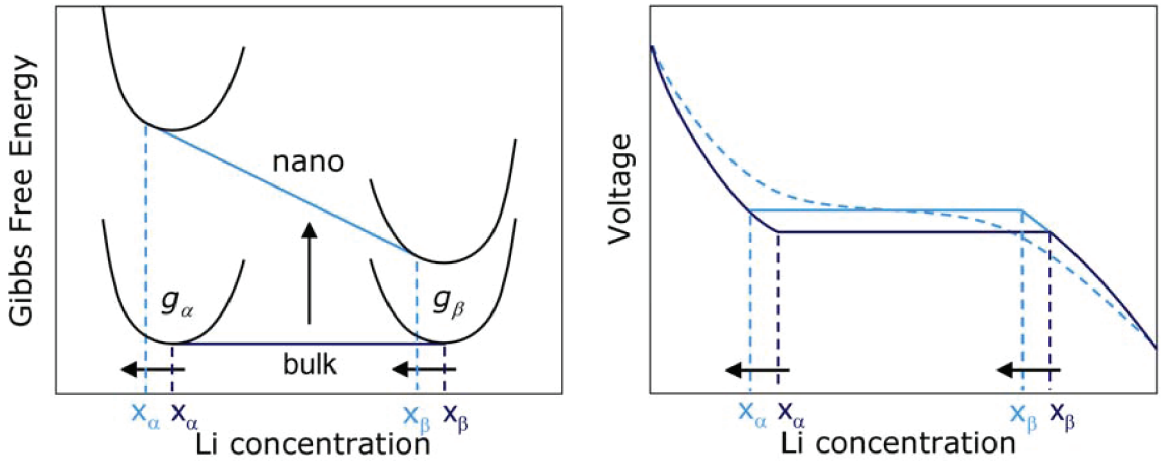

FIGURE 6. Schematic impact of the surface energy on the Gibbs Free energy and voltage profile of an insertion material exhibiting a first-order phase transition upon (de)lithiation. A difference in surface energy leads to a different free energy that scales with the particle surface area. The consequence is a change in the chemical potential and hence in voltage plateau and a shift in the solubility limits. A distribution in particle sizes leads to a distribution of voltages as shown by the dotted voltage profile.

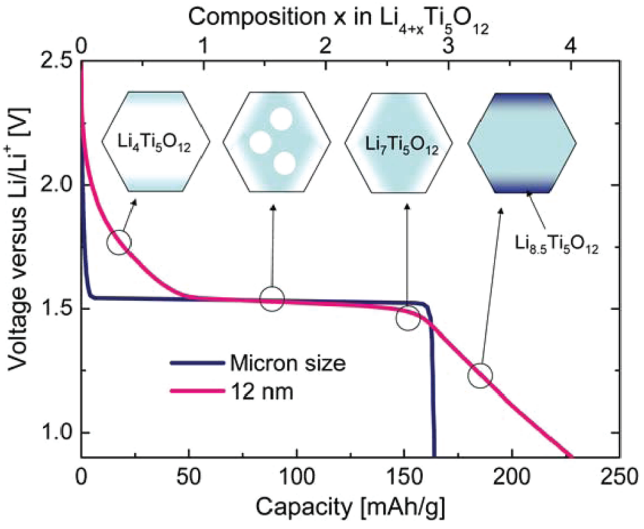

FIGURE 7. Illustration of the suggested origin of the curved voltage profile and enhanced capacity in nanosized LTO.

when the particle size is reduced, see Figure 2 and 7. It suggests that specific surfaces accommodate lithium storage that exceeds the maximum bulk compositions $Li_{0.5}TiO_2$[4,11] and $Li_7Ti_5O_{12}$.[5,52,53] Unlike in bulk material, this leads to capacities close to the theoretical value based on the Ti^{3+}/Ti^{4+} redox couple. A potential explanation is that oxygen termination in combination with surface relaxation allows additional lithium storage at a lower energy, and hence at a higher voltage compared with the bulk. The higher storage capacities of surfaces can potentially be tuned by controlling size and shape of the particles. However, this can also have a down side since in LTO these large surface compositions lead to surface reconstruction and irreversible capacity loss.[5,59]

The clear disadvantage of the large surface area of nanosized materials is parasitic side reactions at the interface with the electrolyte. Because the voltages of the transition metal oxides and phosphates are well above 0.8 V, reductive SEI formation in these materials is not the main concern. Specifically for the titanium oxides the finding of Ti−O−H reacting toward Ti−O−Li species in high surface area nanoamorphous TiO_2[42] is most likely the reason that all proton-containing titanium oxides suffer from an irreversible capacity loss that scales with the surface area during the first discharge.

The intended advantage of nanostructured insertion electrodes is the shortening of the diffusion distance through the solid state, since solid state diffusion is relatively sluggish compared with the diffusion through the liquid electrolyte. An additional advantage may be the induced changes in solubility limits by nanosizing, introducing higher degrees of vacancies or interstitials, enabling higher intrinsic lithium mobility. In nanosized titanium oxides a promise is the larger capacity due to near surface storage, toward fully utilizing the Ti^{3+}/Ti^{4+} redox couple. Another advantage is the increasing amount of charge in the electrochemical double layer, usually referred to as supercapacitive behavior. These aspects suggest a higher power density for nanoscaled electrodes. However, at high rates the electrolyte in the pores of the electrodes may become rate limiting, and although high porosity may prevent this, the latter would lead to an undesired decrease of the overall energy density, and a poorer electronic wiring of the electrode.[58] The consequence is that only a relatively small fraction of the

nanostructured material will participate during fast (dis)-charge, mitigating the advantages of nanosized materials. To utilize the favorable properties of nanomaterials, strategies need to be developed that optimize the ionic transport through the electrolyte toward the electrode particles.[9]

We conclude that although the relatively young field of nanoionics has shown significant promise, many challenges remain to further exploit the large potential for safe and concentrated Li-ion storage in insertion electrodes. Smart use of the surprising and favorable effects, and at the same time minimizing the disadvantages of nanoscaling, is essential.

BIOGRAPHICAL INFORMATION

Marnix Wagemaker received his Ph.D. from the Delft University of Technology in 2003 on lithium storage and dynamics in anatase TiO_2. He received Veni and Vidi grants in 2004 and 2007 on the impact of nanosizing on insertion compounds and is currently appointed assistant professor at the Delft University of Technology. His research interest is fundamental properties and mechanisms in Li-ion storage materials.

Fokko Mulder received his Ph.D. in physics on nanometallic and magnetic systems from Leiden University in 1994. After a post-doctoral position at the Leiden Institute of Chemistry on structure and dynamics of advanced polymer materials, he became researcher at the TU Delft. In 2008, he became full professor on the chair Materials for Integrated Energy Systems within the 3TU. Centre for Sustainable Energy Technologies formed by the Dutch technical universities.

REFERENCES

1 Maier, J. Nanoionics: Ion transport and electrochemical storage in confined systems. *Nat. Mater.* **2005**, *4* (11), 805–815.

2 Arico, A. S.; Bruce, P.; Scrosati, B.; Tarascon, J. M.; Van Schalkwijk, W. Nanostructured materials for advanced energy conversion and storage devices. *Nat. Mater.* **2005**, *4* (5), 366–377.

3 Meethong, N.; Huang, H. Y. S.; Carter, W. C.; Chiang, Y. M. Size-dependent lithium miscibility gap in nanoscale Li1-xFePO4. *Electrochem. Solid-State Lett.* **2007**, *10* (5), A134–A138.

4 Sudant, G.; Baudrin, E.; Larcher, D.; Tarascon, J. M. Electrochemical lithium reactivity with nanotextured anatase-type TiO2. *J. Mater. Chem.* **2005**, *15* (12), 1263–1269.

5 Borghols, W. J. H.; Wagemaker, M.; Lafont, U.; Kelder, E. M.; Mulder, F. M. Size effects in the $Li_{4+x}Ti_5O_{12}$ spinel. *J. Am. Chem. Soc.* **2009**, *131* (49), 17786–17792.

6 Kobayashi, G.; Nishimura, S. I.; Park, M. S.; Kanno, R.; Yashima, M.; Ida, T.; Yamada, A. Isolation of solid solution phases in size-controlled LixFePO4 at room temperature. *Adv. Funct. Mater.* **2009**, *19* (3), 395–403.

7 Wagemaker, M.; Borghols, W. J. H.; Mulder, F. M. Large impact of particle size on insertion reactions, A case of anatase Li_xTiO_2 . *J. Am. Chem. Soc* **2007**, *129*, 4323.

8 Wagemaker, M.; Singh, D. P.; Borghols, W. J. H.; Lafont, U.; Haverkate, L.; Peterson, V. K.; Mulder, F. M. Dynamic solubility limits in nanosized olivine $LiFePO_4$. *J. Am. Chem. Soc.* **2011**, *133* (26), 10222–10228.

9 Kang, B.; Ceder, G. Battery materials for ultrafast charging and discharging. *Nature* **2009**, *458* (7235), 190–193.

10 Hu, Y. S.; Kienle, L.; Guo, Y. G.; Maier, J. High lithium electroactivity of nanometer-sized rutile TiO_2. *Adv. Mater.* **2006**, *18* (11), 1421–1426.

11 Gao, X. P.; Lan, Y.; Zhu, H. Y.; Liu, J. W.; Ge, Y. P.; Wu, F.; Song, D. Y. Electrochemical performance of anatase nanotubes converted from protonated titanate hydrate nanotubes. *Electrochem. Solid-State Lett.* **2005**, *8* (1), A26–A29.

12 Armstrong, A. R.; Armstrong, G.; Canales, J.; Garcia, R.; Bruce, P. G. Lithium-ion intercalation into TiO_2-B nanowires. *Adv. Mater.* **2005**, *17* (7), 862–865.

13 Balaya, P.; Li, H.; Kienle, L.; Maier, J. Fully reversible homogeneous and heterogeneous Li storage in RuO2 with high capacity. *Adv. Funct. Mater.* **2003**, *13* (8), 621–625.

14 Schimmel, H. G.; Huot, J.; Chapon, L. C.; Tichelaar, F. D.; Mulder, F. M. Hydrogen cycling of niobium and vanadium catalyzed nanostructured magnesium. *J. Am. Chem. Soc.* **2005**, *127* (41), 14348–14354.

15 Borghols, W. J. H.; Wagemaker, M.; Lafont, U.; Kelder, E. M.; Mulder, F. M. Impact of nanosizing on lithiated rutile TiO_2. *Chem. Mater.* **2008**, *20* (9), 2949–2955.

16 Padhi, A. K.; Nanjundaswamy, K. S.; Goodenough, J. B. Phospho-olivines as positive-electrode materials for rechargeable lithium batteries. *J. Electrochem. Soc.* **1997**, *144* (4), 1188–1194.

17 Chung, S. Y.; Bloking, J. T.; Chiang, Y. M. Electronically conductive phospho-olivines as lithium storage electrodes. *Nat. Mater.* **2002**, *1* (2), 123–128.

18 Huang, H.; Yin, S. C.; Nazar, L. F. Approaching theoretical capacity of LiFePO4 at room temperature at high rates. *Electrochem. Solid-State Lett.* **2001**, *4* (10), A170–A172.

19 Delacourt, C.; Poizot, P.; Levasseur, S.; Masquelier, C. Size effects on carbon-free LiFePO4 powders. *Electrochem. Solid-State Lett.* **2006**, *9* (7), A352–A355.

20 Meethong, N.; Huang, H. Y. S.; Speakman, S. A.; Carter, W. C.; Chiang, Y. M. Strain accommodation during phase transformations in olivine-based cathodes as a materials selection criterion for high-power rechargeable batteries. *Adv. Funct. Mater.* **2007**, *17* (7), 1115–1123.

21 Wagemaker, M.; Mulder, F. M.; van der Ven, A. The role of surface and interface energy on phase stability of nanosized insertion compounds. *Adv. Mater.* **2009**, *21*, 1–7.

22 Burch, D.; Bazant, M. Z. Size-dependent spinodal and miscibility gaps for intercalation in nanoparticles. *Nano Lett.* **2009**, *9* (11), 3795–3800.

23 Jamnik, J.; Maier, J. Nanocrystallinity effects in lithium battery materials - Aspects of nano-ionics. Part IV. *Phys. Chem. Chem. Phys.* **2003**, *5* (23), 5215–5220.

24 Van der Ven, A.; Wagemaker, M. Effect of surface energies and nano-particle size distribution on open circuit voltage of Li-electrodes. *Electrochem. Commun.* **2009**, *11* (4), 881–884.

25 Delacourt, C.; Poizot, P.; Tarascon, J. M.; Masquelier, C. The existence of a temperature-driven solid solution in LixFePO4 for $0 \leq x \leq 1$. *Nat. Mater.* **2005**, *4* (3), 254–260.

26 Zhou, F.; Marianetti, C. A.; Cococcioni, M.; Morgan, D.; Ceder, G. Phase separation in Li_xFePO_4 induced by correlation effects. *Phys. Rev. B* **2004**, *69*, No. 201101.

27 Yamada, A.; Koizumi, H.; Nishimura, S. I.; Sonoyama, N.; Kanno, R.; Yonemura, M.; Nakamura, T.; Kobayashi, Y. Room-temperature miscibility gap in LixFePO4. *Nat. Mater.* **2006**, *5* (5), 357–360.

28 Dodd, J. L.; Yazami, R.; Fultz, B. Phase diagram of Li(x)FePO4. *Electrochem. Solid-State Lett.* **2006**, *9* (3), A151–A155.

29 Stevens, R.; Dodd, J. L.; Kresch, M. G.; Yazami, R.; Fultz, B.; Ellis, B.; Nazar, L. F. Phonons and thermodynamics of unmixed and disordered $Li_{0.6}FePO_4$. *J. Phys. Chem. B* **2006**, *110* (45), 22732–22735.

30 Van der Ven, A.; Garikipati, K.; Kim, S.; Wagemaker, M. The role of coherency strains on phase stability in LixFePO4: Needle crystallites minimize coherency strain and overpotential. *J. Electrochem. Soc.* **2009**, *156* (11), A949–A957.

31 Singh, G. K.; Ceder, G.; Bazant, M. Z. Intercalation dynamics in rechargeable battery materials: General theory and phase-transformation waves in LiFePO4. *Electrochim. Acta* **2008**, *53* (26), 7599–7613.

32 Delmas, C.; Maccario, M.; Croguennec, L.; Le Cras, F.; Weill, F. Lithium deintercalation in LiFePO4 nanoparticles via a domino-cascade model. *Nat. Mater.* **2008**, *7* (8), 665–671.

33 Chen, G. Y.; Song, X. Y.; Richardson, T. J. Electron microscopy study of the LiFePO4 to FePO4 phase transition. *Electrochem. Solid-State Lett.* **2006**, *9* (6), A295–A298.

34 Laffont, L.; Delacourt, C.; Gibot, P.; Wu, M. Y.; Kooyman, P.; Masquelier, C.; Tarascon, J. M. Study of the $LiFePO_4/FePO_4$ two-phase system by high-resolution electron energy loss spectroscopy. *Chem. Mater.* **2006**, *18* (23), 5520–5529.

35 Kavan, L.; Kalbac, M.; Zukalova, M.; Exnar, I.; Lorenzen, V.; Nesper, R.; Graetzel, M. Lithium storage in nanostructured TiO_2 made by hydrothermal growth. *Chem. Mater.* **2004**, *16* (3), 477–485.

36 Yang, Z. G.; Choi, D.; Kerisit, S.; Rosso, K. M.; Wang, D. H.; Zhang, J.; Graff, G.; Liu, J. Nanostructures and lithium electrochemical reactivity of lithium titanites and titanium oxides: A review. *J. Power Sources* **2009**, *192* (2), 588–598.

37 Reddy, M. A.; Kishore, M. S.; Pralong, V.; Varadaraju, U. V.; Raveau, B. Lithium intercalation into nanocrystalline brookite TiO2. *Electrochem. Solid-State Lett.* **2007**, *10* (2), A29–A31.

38 Zukalova, M.; Kalbac, M.; Kavan, L.; Exnar, I.; Graetzel, M. Pseudocapacitive lithium storage in TiO_2(B). *Chem. Mater.* **2005**, *17* (5), 1248–1255.

39 Cava, R. J.; Murphy, D. W.; Zahurak, S.; Santoro, A.; Roth, R. S. The crystal-structures of the lithium-inserted metal-oxides Li0.5TiO2 Anatase, LiTi2O4 spinel, and Li2Ti2O4. *J. Solid State Chem.* **1984**, *53* (1), 64–75.

40 Wagemaker, M.; Kearley, G. J.; van Well, A. A.; Mutka, H.; Mulder, F. M. Multiple Li positions inside oxygen octahedra in lithiated TiO_2 anatase. *J. Am. Chem. Soc.* **2003**, *125* (3), 840–848.

41 Borghols, W. J. H.; Wagemaker, M.; Laffont, U.; Kelder, E. M.; Mulder, F. M. Impact of nanosizing on lithiated rutile TiO_2. *Chem. Mater.* **2008**, *20*, 2949–2955.

42 Borghols, W. J. H.; Lutzenkirchen-Hecht, D.; Haake, U.; Chan, W.; Lafont, U.; Kelder, E. M.; van Eck, E. R. H.; Kentgens, A. P. M; Mulder, F. M.; Wagemaker, M. Lithium storage in amorphous TiO2 nanoparticles. *J. Electrochem. Soc.* **2010**, *157* (5), A582–A588.

43 Li, H.; Shi, L. H.; Lu, W.; Huang, X. J.; Chen, L. Q. Studies on capacity loss and capacity fading of nanosized SnSb alloy anode for Li-ion batteries. *J. Electrochem. Soc.* **2001**, *148* (8), A915–A922.

44 Aurbach, D.; Markovsky, B.; Weissman, I.; Levi, E.; Ein-Eli, Y. On the correlation between surface chemistry and performance of graphite negative electrodes for Li ion batteries. *Electrochim. Acta* **1999**, *45* (1−2), 67–86.

45 Ferg, E.; Gummow, R. J.; Dekock, A.; Thackeray, M. M. Spinal anodes for lithium-ion batteries. *J. Electrochem. Soc.* **1994**, *141* (11), L147–L150.

46 Murphy, D. W.; Cava, R. J.; Zahurak, S. M.; Santoro, A. Ternary LixTiO2 Phases from Insertion Reactions. *Solid State Ionics* **1983**, *9−10* (Dec), 413–417.

47 Colbow, K. M.; Dahn, J. R.; Haering, R. R. Structure and Electrochemistry of the Spinel Oxides LiTi2O4 and Li4/3Ti5/3O4. *J. Power Sources* **1989**, *26* (3−4), 397–402.

48 Scharner, S.; Weppner, W.; Schmid-Beurmann, P. Evidence of two-phase formation upon lithium insertion into the Li1.33Ti1.67O4 spinel. *J. Electrochem. Soc.* **1999**, *146* (3), 857–861.

49 Wagemaker, M.; Simon, D. R.; Kelder, E. M.; Schoonman, J.; Ringpfeil, C.; Haake, U.; Lützenkirchen-Hecht, D.; Frahm, R.; Mulder, F. M. A kinetic two-phase and equilibrium solid solution in spinel Li4+xTi5O12. *Adv. Mater.* **2006**, *18* (23), 3169–3173.

50 Wagemaker, M.; van Eck, E. R. H.; Kentgens, A. P. M; Mulder, F. M. Li-ion diffusion in the equilibrium nanomorphology of spinel $Li_{4+x}Ti_5O_{12}$. *J. Phys. Chem. B* **2009**, *113* (1), 224–230.

51 Kavan, L.; Prochazka, J.; Spitler, T. M.; Kalbac, M.; Zukalova, M. T.; Drezen, T.; Gratzel, M. Li insertion into Li4Ti5O12 p(Spinel) - Charge capability vs. particle size in thin-film electrodes. *J. Electrochem. Soc.* **2003**, *150* (7), A1000–A1007.

52 Ge, H.; Li, N.; Li, D. Y.; Dai, C. S.; Wang, D. L. Electrochemical characteristics of spinel Li4Ti5O12 discharged to 0.01 V. *Electrochem. Commun.* **2008**, *10* (5), 719–722.

53 Zhong, Z. Y.; Ouyang, C. Y.; Shi, S. Q.; Lei, M. S. Ab initio studies on Li4+xTi5O12 compounds as anode materials for lithium-ion batteries. *ChemPhysChem* **2008**, *9* (14), 2104–2108.

54 Hill, T. L. *Thermodynamics of Small Systems*; W.A. Benjamin: New York, 1963.

55 Dreyer, W.; Jamnik, J.; Guhlke, C.; Huth, R.; Moskon, J.; Gaberscek, M. The thermodynamic origin of hysteresis in insertion batteries. *Nat. Mater.* **2010**, *9* (5), 448–453.

56 Ganapathy, S.; Wagemaker, M. A first principles study on surface effects for lithium intercalation in spinel lithium titanium oxides. *J. Am. Chem. Soc.* Submitted for publication.

57 Chen, J. S.; Tan, Y. L.; Li, C. M.; Cheah, Y. L.; Luan, D. Y.; Madhavi, S.; Boey, F. Y. C.; Archer, L. A.; Lou, X. W. Constructing hierarchical spheres from large ultrathin anatase TiO_2 nanosheets with nearly 100% exposed (001) facets for fast reversible lithium storage. *J. Am. Chem. Soc.* **2010**, *132* (17), 6124–6130.

58 Fongy, C.; Gaillot, A. C.; Jouanneau, S.; Guyomard, D.; Lestriez, B. Ionic vs Electronic Power Limitations and Analysis of the Fraction of Wired Grains in LiFePO4 Composite Electrodes. *J. Electrochem. Soc.* **2010**, *157* (7), A885–A891.

59 Hirayama, M.; Kim, K.; Toujigamori, T.; Cho, W.; Kanno, R. Epitaxial growth and electrochemical properties of $Li_4Ti_5O_{12}$ thin-film lithium battery anodes. *Dalton Trans.* **2011**, *40*, 2882–2887.